

Glycolaldehyde as a Bio-Based C₂ Platform Chemical: Catalytic Reductive Amination of Vicinal Hydroxyl Aldehydes

William Faveere,[†] Tzvetan Mihaylov,[‡] Michiel Pelckmans,[†] Kristof Moonen,[§] Frederik Gillis-D'Hamers,[†] Roel Bosschaerts,^{||} Kristine Pierloot,[‡] and Bert F. Sels^{*,†}

[†]Center for Sustainable Catalysis and Engineering (CSCE), Department M²S, KU Leuven, Celestijnenlaan 200F, 3001 Leuven, Belgium

[‡]Department of Chemistry, KU Leuven, Celestijnenlaan 200F, 3001 Leuven, Belgium

[§]Eastman Chemical Company, Technologiepark 21, 9052 Zwijnaarde, Belgium

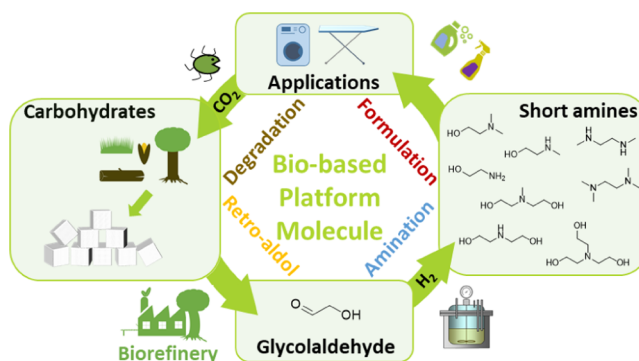
^{||}Ecover, Industrieweg 3, 2390 Malle, Belgium

S Supporting Information

ABSTRACT: Reductive amination of glycolaldehyde (GA), the smallest sugar molecule and obtainable from biomass, creates a versatile platform for ethylamine products, potentially replacing current pathways via toxic ethylene oxide and dichloroethane. Given the high reactivity of α -OH carbonyls, the main challenge was control of selectivity in a cascade of parallel and consecutive reactions during reductive amination. The type of solvent and catalyst, preferably methanol and Pd, respectively, are key enabling parameters to achieve high product yields. A kinetic study on product intermediates accompanied with detailed product analysis (MS and NMR) suggested a general mechanistic scheme and validation with density functional theory calculations provided

a rational understanding of the solvent effect in terms of energetics and kinetics. Primary alkanolamines (AA) such as 2-(dimethylamino)-ethanol are preferred products, and large excess of the amine reagent is not required to reach almost quantitative yields. Interestingly substoichiometric amine-to-GA ratio allows for high yield of higher (consecutive) AAs such as *N*-methyldiethanolamine (MDEA) and triethanolamine, for which a peculiar cyclic 5-membered oxazolidinic precursor was analyzed (e.g., for reaction with monomethylamine to MDEA). The shift to diamine-selective (DA) reactions is possible by switching to a two-step one-pot approach. With ethylene glycol as a preferred solvent, high yield of an unsaturated C₂-enediamine precursor is obtained under an inert atmosphere, followed by its metal-catalyzed hydrogenation at elevated temperature to the final DA product such as *N,N,N',N'*-tetramethylethylene-diamine. A conceptual model of the catalytic reductive amination routes that allows production of a variety of ethylamines with up to +90 C % yield is thus presented. The successful preparation and sensory assessment of a GA-based diester quat in fabric softener formulations demonstrates the viability of a full bio-based and drop-in production route for high-value chemicals, directly from GA as a platform molecule.

KEYWORDS: glycolaldehyde, biomass, heterogeneous catalysis, reductive amination, DFT, reaction mechanism, alkanolamine, ethylene diamine



INTRODUCTION

Today's chemical industry is producing low molecular weight alkanolamines (AAs) and ethylene diamines (DAs) by reaction of oxiranes or chlorinated hydrocarbons and ammonia, primary or secondary amines.¹ The AAs are commonly used as scrubbing agents for acid gasses like CO₂ and H₂S,² or as intermediates for surfactants,³ cosmetics,⁴ and pharmaceuticals.⁵ DAs have applications as curing agents in epoxy resins and as catalysts in the polyurethane synthesis.⁶ The current production method of the C₂ AAs and DAs specifically involves epoxidation or chlorination of oil-based ethylene, respectively. Use of bioethanol may result in a more sustainable synthesis route, though involvement of the toxic

intermediates (IM), ethylene oxide (EO), and dichloroethane (DCE), and the rigorous safety precautions associated with them lowers the green chemistry and sustainability impact of these amine production routes.⁷ Investigation of new sustainable routes toward these valuable amines is therefore desirable.⁸

Glycolaldehyde (GA) is the smallest molecule in the homologous series of reducing sugars and it may have great potential to act as a renewable and safer alternative for C₂

amine synthesis. It is abundantly present in biomass pyrolysis oil, and its toxicity is significantly lower than that of EO and DCE.^{9,10} Worldwide research is ongoing to improve its synthesis from biomass, while its potential use as platform chemical is being demonstrated. Promising research into bio-based GA production routes includes pyrolysis,^{11,12} supercritical water treatment,¹³ catalytic retro-aldol reactions,^{14,15} and hydrous thermolysis of glucose^{16,17} which can be exerted further without prior isolation. For instance, it is generally known that GA is the key intermediate (IM) in the production of renewable ethylene glycol (EG) from carbohydrates.^{14,18–22} Haldor Topsoe and Braskem collaborate on the production of sugar-based GA by hydrous thermolysis on a demonstration scale, currently ongoing.^{23,24} Furthermore, our group and others demonstrated a selective reductive aminolysis of sugars forming short amines at low temperature, in which the role of GA as key IM was revealed.^{25–27} Besides the C₂ amines and EG, GA can also undergo selective oxidation to glycolic acid,²⁸ or aldol and polymerization reactions to create new polymer building blocks.^{29–33} In the field of GA amination, Zhang and co-workers recently reported formation of C₂-amines straight from cellulosic biomass in a two-step process, yielding 10% monoethanolamine (MEOA). They followed a unique approach by first performing an acid-catalyzed hydrolysis of cellulose and retro-aldol of glucose into GA, followed by the reductive amination of GA with NH₃ in water.^{27,34}

Control of selectivity is the major concern in the reductive amination of aldehydes and ketones, and it is particularly challenging with α -hydroxy substrates such as GA.^{35,36} Carbonyls are intrinsically susceptible for nucleophilic addition (e.g., with alcohols or water) and for aldol reactions. In reductive amination circumstances, the reactive carbonyl group can also reduce to the alcohol, causing depletion of substrate. As well, the carbonyl may react with the present amine, creating a reactive imine (or enamine with secondary amine reagents) that can undergo condensation forming a mixture of primary, secondary, and/or tertiary amines as well as cyclic products such as piperazines, upon hydrogenation. Especially, the α -OH imine/enamine IM is very susceptible for so-called Maillard reactions³⁷ and caramelization³⁸ (generally recognized in the food industry), Amadori rearrangements³⁹ and keto-enol tautomerisation,⁴⁰ giving rise to a vast array of complex side-products which darken the reaction mixture.

The above product selectivity issue, thus expectedly most problematic with α -OH carbonyls, has forced practical amine synthesis through the use of epoxides, chlorinated hydrocarbons, and alcohols, the latter being dehydrogenated in situ to the carbonyl group in the presence of a metal catalyst, preferably assisted by a soluble base.⁴¹

There is common knowledge, already applied for the amination of EO, to improve the selectivity of reductive amination.³⁶ For instance, an excess of amine reagent is necessary to facilitate high selectivity toward primary amine products.^{1,42} A second control of selectivity implies the hydrogenation capacity of the metal catalyst; hydrogenation must occur fast enough to stabilize the imine/enamine into the corresponding amine, thereby avoiding side-reactions, but the reaction must be sufficiently slow as to allow imine/enamine formation from the carbonyl.

The challenge for selective GA amination can thus be found in understanding and balancing the different parameters that control reaction selectivity. Here, we report the first systematic study of the catalyst, solvent and, reaction conditions for the

reductive amination of GA with ammonia and commercial methyl amines, to achieve both high DA and AA product yields. The reaction rate and selectivity are rationalized at the atomistic level, taking into account a mechanistic proposal, experimental kinetic data, and theoretical calculations. An illustrative valorization of one of the AA products as potential building block for a renewable fabric softener is reported.

■ EXPERIMENTAL SECTION

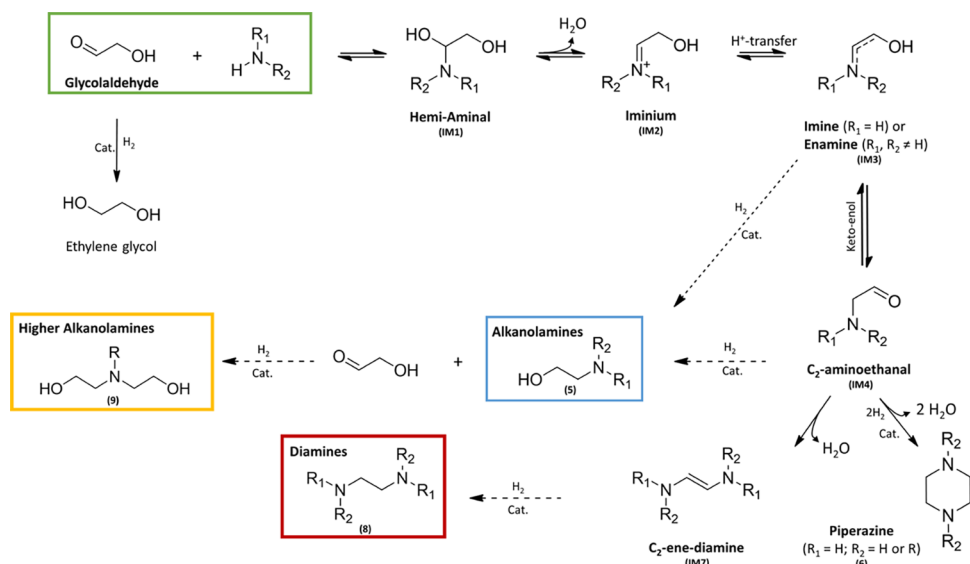
Reagents and Catalysts. Chemicals: NH₃ 4 M in MeOH; monomethylamine (MMA) 40 wt % aq; MMA 2 M in MeOH, 2 M in tetrahydrofuran (THF) and 5.6 M in EtOH; dimethylamine (DMA) 40 wt % aq; DMA 2 M in MeOH, 2 M in THF and 5.6 M in EtOH; GA dimer; triethylene glycol dimethyl ether; DMSO-*d*₆; deuterated chloroform; palmitoyl chloride; HF 40 wt % (Sigma-Aldrich). Ethanol; dichloromethane (Fischer Chemical Ltd.). Kalium chloride, sodiumbicarbonate (Chemlab). Triethylamine (Acros). Catalysts and supports: Pd/C (5 wt %), Ru/C (5 wt %), 65 wt % Ni/SiO₂Al₂O₃ (Sigma-Aldrich). Ni-6458P (56 wt %) (Engelhard). Raney Ni-5601; Raney Co-2724 (Grace).

Reaction, Instrumentation, and Analysis. Reactions were performed in a 50 mL high-pressure batch reactor (Parr, 5500 series), equipped with mechanical stirring and automated temperature and pressure monitoring. For a typical reaction, 0.5 g of GA dimer, 0.13 g of catalyst (1.5 wt % of the total reaction mixture), 0.2 g of triethylene glycol dimethyl ether [internal standard (IS) for analysis], and a specified volume of solvent and amine were added to the reactor (for details see captions). After closing, the reactor was flushed with N₂, pressurized with H₂ to 70 bar at room temperature (RT), and heated (with a rate of 4 °C/min) to 100 °C, and stirred at 800 rpm for a total time of 1 h. After reaction, an ice bath was used to cool the reactor to RT. The reaction product including the catalyst was centrifuged and the supernatant was used for product analysis. ¹³C NMR with deuterated dimethylsulfoxide (DMSO-*d*₆) and GC-MS were used for identification of the products. GC-analysis with triethylene glycol dimethyl ether as an IS was finally used for product yield quantification.

The appearance of key IM's prior to hydrogenation was noticed by analyzing the product mixture during the course of the reductive amination reaction, and the products were identified as the C₂-ene-diamine (in case of DMA) and a 5-membered oxazolidinic ring structure (in case of sub-stoichiometric MMA-to-GA molar ratio) by means of GC-MS and ¹³C NMR (see the [Supporting Information](#)). Monitoring the solvent-dependent formation of these IMs was done in a separate experiment, in which an amount of GA, amine, IS, and selected solvent were mixed in a GC vial at RT (no catalyst involved), and the IM formation (and disappearance) kinetics were followed through on-line GC analysis by injection of the sample every 10 min. Because the IMs are not commercially available, a GC response factor relative to the IS was estimated using the ECN analysis.⁴³ Based on the formation kinetics, a two-step one-pot synthesis procedure was developed to exploit and maximize the formation of the C₂-ene-diamine IM. A reaction mixture of GA, DMA, IS, and solvent was stirred at RT under 40 bar of N₂ for a chosen time, before the catalyst was added in the second step, pressurized with H₂, and brought to reaction conditions.

Density Functional Theory Calculations. All calculations were performed with the hybrid meta-GGA functional

Scheme 1. Proposed Reaction Scheme for the Reductive Amination of GA



M062X-D3⁴⁴ and 6-311+G(2df,2p) basis sets, using the Gaussian 09 software package.⁴⁵ The bulk solvent effects were included in the geometry optimizations by means of the integral equation formalism polarizable continuum model (IEFPCM)^{46,47} with the default UFF atomic radii. A limited number of explicit solvent molecules, n , were also added into the models, as n was varied in order to minimize the energy barriers.⁴⁸ Such an approach has been shown to be appropriate for studying organic and organometallic reactions in solution.⁴⁹ To confirm the character of all first-order saddle points and minima on the potential energy surface (PES) and to obtain the thermochemical data, vibrational frequency calculations were carried out using the standard rigid rotor-harmonic oscillator approximation. Intrinsic reaction coordinate calculations were also performed to verify that the located transition states (TSs) connect the expected minima on the PES. The liquid phase free energy (G_{liq}^*) of the species was estimated as

$$G_{\text{liq}}^* = G^0 + \Delta G_{\text{sol}}^* + \Delta G^{0 \rightarrow *}$$
 (1)

where G^0 is the gas-phase free energy (1 atm, 298.15 K), ΔG_{sol}^* is the free energy of solvation (as derived from IEFPCM model), and $\Delta G^{0 \rightarrow *} = RT \ln(24.46)$ is the standard state correction accounting for the free-energy change of 1 mol of ideal gas from 1 atm (24.46 L mol⁻¹) to 1 mol L⁻¹.⁵⁰ At 298.15 K, $\Delta G^{0 \rightarrow *}$ is 1.89 kcal mol⁻¹. An extra term, $RT \ln([S])$,⁵⁰ was added to the G_{liq}^* of explicitly treated solvent molecules to account for the free-energy change associated with the change in concentration from 1 mol L⁻¹ to the standard-state concentration of the solvent in the liquid phase [S]. At 298.15 K, [S] is 55.3, 17.9, and 24.7 mol L⁻¹ for water, EG, and methanol, respectively.

Preparation of Esterquats. Esterification of the components *N*-methyldiethanolamine (MDEA) and *N,N'*-bis(2-hydroxyethyl)-*N,N'*-dimethyl-ethylenediamine (BHEDMEDA), obtained from this contribution and the work of Pelckmans et al., respectively, was performed with palmitoyl chloride following the procedure of Chandrashekhara et al.^{25,51} In case of MDEA, a stoichiometric amount of 5 g palmitoyl chloride (C16:0) was dissolved in 25 mL of dichloromethane under inert conditions. Next, 1 g of MDEA was added, followed by a dropwise addition of triethylamine on ice. After

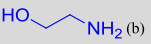

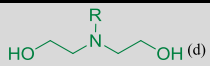
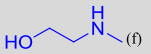

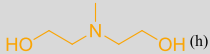
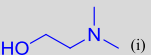

stirring overnight, the remaining dichloromethane was evaporated on a rotavap and the product was re-dissolved in 50 mL of dichloromethane. The solution was washed with salt solutions of 5% sodium bicarbonate (3 times) and 5% potassium chloride (2 times), each time with removal of the top aqueous layer. After evaporation, the final product was solidified, and the purity was analyzed using ¹H NMR with deuterated chloroform as NMR solvent. Subsequent quaternization of the final MDEA diester was carried out after De Vos et al. with methyl chloride as a methylating agent and confirmed with ¹³C NMR and deuterated chloroform as the NMR solvent (see the Supporting Information).⁵²

Fabric Softener Test Procedure. Two different esterquats, obtained via the procedure above (MDEA and BHEDMEDA), and a commercial TEA-based standard (structure see the Supporting Information) were formulated into a fabric softener.²⁶ A batch of standardized towels were prehardened by washing them four times with an industrial detergent (IEC-A base detergent; non-perfumed) at 90 °C to remove all possible residues. Identical settings, loading, and dosing were applied for all laundry cycles. Next, four towels were treated per fabric softener formulation (5 wt % MDEA, 5 wt % BHEDMEDA, 5 wt % TEA, 3 wt % TEA and a blank in soft water). An experienced test panel of eight people were asked to rank the towels from softest to hardest in a sensory assessment, according to ISO-8587:2006. Significant differences ($P < 0.05$) between the formulations were determined by a hierarchy test combined with pair-wise testing between formulations, following the statistical method as described by Kramer et al. (see the Supporting Information).⁵³

RESULTS

Catalyst and Parameter Screening in Aqueous Conditions. Classic reductive amination of aldehydes under a H₂ atmosphere with ammonia, primary, and secondary amines requires a metal catalyst that reduces the imine and enamine IM, respectively, into the final product. Considering the aforementioned selectivity challenges of α -OH aldehyde amination, additional fast tautomerization may occur at the level of the imine or enamine IM, allowing a second amination step. Two key products, AAs and DAs, are hence expected (see

Table 1. Screening of Noble and Non-Noble Metal Heterogeneous Catalysts for the Reductive Amination of GA with Aqueous Amine Solutions^a

#	Catalyst	AA [C%]	DA [C%]	Higher AA [C%]	Mass Balance [C%]	
		NH₃/GA				
1a	Ni-6458P (56 wt.%)	4	15	0	0	15
1b	Ni-6458P (56 wt.%)	35	45	0	0	45
2	Raney® Co-2724 ^(e)	8	35	0	0	35
		MMA/GA				
3	Ni/SiO ₂ -Al ₂ O ₃ (65 wt.%)	8	79	5	0	84
4a	Ni-6458P (56 wt.%)	1	17	3	0	20
4b	Ni-6458P (56 wt.%)	2	22	8	0	30
4c	Ni-6458P (56 wt.%)	4	65	15	0	80
4d	Ni-6458P (56 wt.%)	8	85	15	0	100
5	Ni-3354E (60 wt.%)	8	85	13	0	98
6	Ni/kieselguhr (50 wt.%)	8	64	30	0	94
7	Sponge Co + Cr/Ni	8	86	9	0	95
8	Raney® Co-2724 ^(e)	8	92	5	0	97
9a	Pd/C (5 wt.%)	1	40	1	28	70 ^k
9b	Pd/C (5 wt.%)	8	91	5	0	96
10	Ru/C (5 wt.%)	8	86	12	0	100 ^k
		DMA/GA			/	
11	Ni/SiO ₂ -Al ₂ O ₃ (65 wt.%)	8	12	8	/	20
12	Ni-6458P (56 wt.%)	8	4	11	/	15
13	Ni-3354E (60 wt.%)	8	7	14	/	21
14	Ni/kieselguhr (50 wt.%)	8	< 1	5	/	5
15	Sponge Co + Cr/Ni	8	9	10	/	19
16a	Raney® Co-2724 ^(e)	4	16	5	/	21
16b	Raney® Co-2724 ^(e)	8	25	11	/	36
17	Pd/C (5 wt.%)	8	75	7	/	82
18a	Ru/C (5 wt.%)	8	21	24	/	47 ^k
18b	Ru/C (5 wt.%)	1	35	5	/	49 ^k

^aReaction conditions: 0.5 g GA; 0.25 g catalyst; 0.2 g IS; 40 wt % aqueous amine solution, diluted to a reaction mixture of 15 mL at chosen amine-to-GA molar ratio; 100 °C; 70 bar H₂; 1 h reaction. GA conversion = 100%. Mass balance is not complete due to undesired competitive caramelization and/or reactions of the Maillard type. ^bMEOA. ^cEthylenediamine (EDA). ^dDiethanolamine (DEOA) + TEOA. ^ePyrophoric. ^f2-(Methylamino)-ethanol (MAE). ^g*N,N'*-Dimethylethylene-diamine. ^hMDEA. ⁱDMAE. ^jTMEDA. ^kFraction EG is not reported but included in mass balance.

Scheme 1). For instance, the catalytic reductive amination of GA with DMA may form 2-(dimethylamino)ethanol (DMAE) and *N,N,N',N'*-tetramethylethylene-diamine (TMEDA) as desired products.

Cyclic side-products such as piperazines via self-condensation of the imine IM or higher AAs via product condensation with another GA molecule may additionally be formed upon reacting GA with the amines, NH₃ and MMA. In case of MMA, the condensation product, 1,4-dimethylpiperazine, was indeed analyzed in trace amounts (< 1 C %, not included in Table 1), whereas 1,4-piperazine was not detected in the reaction of GA with NH₃.

First, a variety of commercially available heterogeneous metal catalysts were screened with different amines to unveil

their impact on DA to AA selectivity. An amine-to-GA molar ratio of 8 was kept constant (unless otherwise stated) and a standard amount of 1.5 wt % catalyst was used in the aqueous reaction mixture, regardless of the metal loading. The screening results are summarized in Table 1. Because of its high reactivity under reaction conditions, GA conversion was always 100%. Results are reported in carbon % yield (based on initial GA) for all graphs and tables in this contribution. The mass balance was measured to anticipate carbon losses due to oligomer products.

The catalytic data show some clear trends between the different amines and metal catalysts with respect to the total amine product yield. Use of NH₃ exclusively forms the corresponding AA (here, MEOA) (entries 1a, 1b and 2).

However, there is an incomplete mass balance because of competitive side-reactions, viz. condensation, caramelization,³⁸ and Maillard type reactions,³⁷ visible as brown colored product mixtures. Interestingly, reaction of GA with MMA shows higher and sometimes complete mass balance in agreement with the colorless appearance of the product mixtures (entries 3 to 10). The reaction prefers AA (here, 2-(methylamino)-ethanol or MAE) above DA (here, *N,N'*-dimethylethylenediamine or DMEDA) formation, irrespective of the metal catalyst (Co, Ni, Pd, or Ru). In this series of catalysts, only Ni on kieselguhr shows significant amounts of DMEDA, the DA product. Reaction with DMA results in low amine yields, except in presence of Pd, for which a high 82% mass balance was observed (entries 11–19). There is dominant formation of AA (DMAE) over DA (TMEDA) for few catalysts, but this chemoselectivity strongly depends on the metal catalyst and amine-to-GA molar ratio.

Effect of Amine-to-GA Molar Ratio in Aqueous Conditions. Several side reactions may be avoided by increasing the amine-to-GA molar ratio—a strategy commonly applied to, for example, the amination of EO. A higher DA yield may also be expected in large excess of amine. Inversely, a low amine-to-GA molar ratio enables additional condensation of the product with another GA molecule, forming higher AAs such as MDEA in case of MMA. To investigate the amine-to-GA ratio, experiments were conducted with varying amine (here, NH₃ and MMA)-to-GA molar ratio (between 1 and 8, Table 1, entries 1a–b, 4a–d, 9a–b, 18a–b) in the presence of Ni, Pd, or Ru catalyst in water.

Where a total (DA + AA) product yield of only 21% is reached at a GA-to-MMA ratio of 1 with Ni, it rises to completion at ratio 8. Reduction of side reactions at amine excess is visually perceived by the increasing translucency of the product mixture. The reaction is mostly accompanied by a rise in AA selectivity, 2-(methylamino)ethanol (MAE), up to 85%, while an increase in DA yield, DMEDA, (which stoichiometrically needs a higher amine excess) was not observed; its yield shows a plateau at 15%, that already reached at an amine-to-GA molar ratio of 4. A high MMA-to-GA molar ratio with Pd/C results in up to 91% MAE yield. Lowering this ratio is at cost of the carbon mass balance, and this is accompanied with the first observation of higher AAs in aqueous conditions, here MDEA (28%).

Similarly, a high ammonia-to-GA ratio shows better MEOA yields (tested over Ni), but usually much larger amine excess is required with NH₃ to reach high MEOA selectivity. For instance, increasing the ratio from 4 to 35 led to a MEOA yield increase of 15 to 45% (entries 1a and b, Table 1). Mass balance remains far from complete. Reaction of GA with stoichiometric amounts of DMA favors DMAE formation, besides forming some EG, whereas excess of DMA reduces EG formation and increases TMEDA formation at the expense of DMAE (entry 18). Mass balance is again low, ~49%, and independent of the DMA-to-GA ratio.

Effect of Solvent. Reductive amination produces water as a result of dehydration of the hemiaminal IM to form enamine/imine IM (see Scheme 1). Therefore, carrying out the reaction in water-poor circumstances should favor the dehydration steps. In addition, the amine reagents are partially present as ammonium salt in aqueous conditions, reducing its nucleophilicity as a consequence of protonation. Also, the conjugated OH⁻ nucleophile may give rise to additional side reactions. Use of nonaqueous inert solvents such as THF,

instead of water, is often reported as the preferred solvent for reductive amination reactions. For example, in patent U.S. No 8772548B2, THF is used as inert solvent for reductive amination of GA with NH₃ in the presence of a Ni/Cu/Zr-oxide catalyst, yielding up to 82% MEOA at a NH₃-to-GA molar ratio of 35.⁵⁴

Our group recently demonstrated the important effect of protic (nonaqueous) solvents such as MeOH to mediate intramolecular proton transfer (PT) reactions during the reductive aminolysis of reducing sugars, thereby drastically lowering the energy barrier for the initial formation of enamine IM of glucose with DMA.^{26,55} Song et al. reported a similar solvent promoting effect in the reductive amination of normal ketones with Ru/C.⁵⁶ They found high ketone conversion in protic solvents, whereas low conversion was observed in THF. Despite water being protic, it hinders dehydration and subsequent imine formation and is therefore not suited. They also noted fast hydrogenation in alcoholic solvents showing the amine as the main product, whereas hydrogenation being sluggish in THF forms mainly imine IM. The latter was tentatively explained through a strong competitive adsorption of the aprotic polar solvent molecules on the catalytically active hydrogenation sites. These reported observations led us to investigate several solvents for the reductive amination of GA with DMA. The results are summarized and compared with the outcome in pure water in Figure 1 for two noble metal catalysts and one Ni catalyst, selected from Table 1.

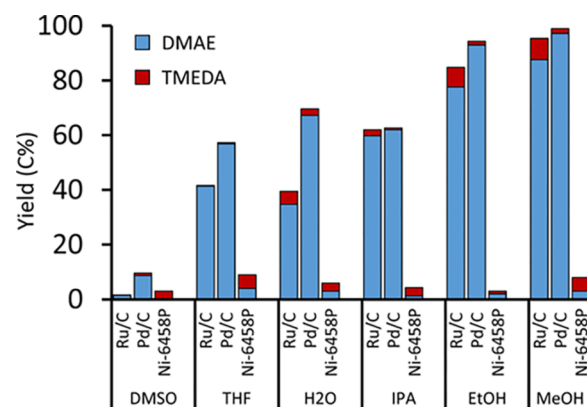


Figure 1. Effect of solvent on the reductive amination of GA. Reaction conditions: 0.5 g GA; 0.13 g catalyst; 0.2 g IS; DMA 2 M in solvent, diluted to 15 mL total at amine-to-GA molar ratio = 1; 100 °C; 70 bar H₂; 1 h reaction time.

Although water as a solvent already results in moderate yields with Pd/C as a catalyst, a solvent-dependent promoting effect on the product yield is prominent in the organic protic solvents, with exceptional 97% DMAE yield obtained in MeOH. No formation of piperazine was detected under these conditions. Notably, the excellent DMAE yields are achieved at stoichiometric DMA-to-GA molar ratio, previously not possible (vide supra). Parallel to earlier observations of Song et al.,⁵⁶ reactions in EtOH showed less impact on the yield, as compared to MeOH, and the use of aprotic solvents such as THF generally results in significantly lower amine yields. A similar solvent-dependent promoting effect, as for Ru and Pd, is surprisingly not observed in presence of Ni. Here, the high amine-to-GA ratio remains crucial to achieve selective amination with a competing mass balance. Only by adding

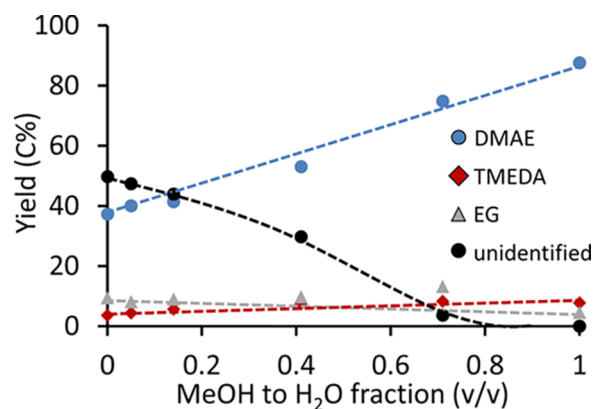


Figure 2. Effect of a gradual methanol addition on the aqueous reductive amination of GA. Reaction conditions: 0.5 g GA; 0.13 g Ru/C; 0.2 g IS; DMA 2 M in solvent, diluted to 15 mL total at amine-to-GA molar ratio = 1; 100 °C; 70 bar H₂; 1 h reaction time. Dashed lines are a guide to the eye.

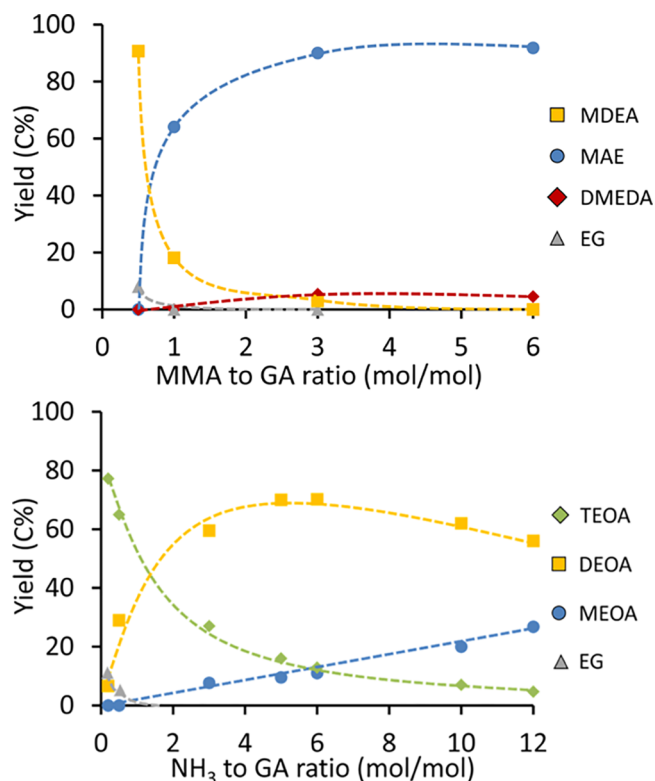


Figure 3. Effect of different amines and molar ratios on the reductive amination of GA. Reaction conditions: 1 g GA; 0.26 g Pd/C; 0.2 g IS; amine 2 M solution in MeOH diluted to 25 mL at a sufficient amine-to-GA molar ratio; 100 °C; 70 bar H₂; 1 h reaction time. Dashed lines are a guide to the eye. Mass balance of all reported products ~95 C % for each amine and ratio.

more catalyst and higher amine-to-GA ratio, considerable amounts of the amine product were formed with Ni, but TMEDA (and not DMAE) is preferably obtained (see later, Figure 5).

The solvent effect was investigated in more detail in the presence of Ru/C by varying the water volume fraction in MeOH over a range from zero to unity. This catalyst was selected to screen the evolution of solvent addition because of its mediocre product yields and no pronounced selectivity to

one of the main products, AA or DA, in water with DMA. As reference, water as the solvent yielded 35 C % DMAE, and about 50 C % of GA-derived products were unidentified, likely the result of undesired Maillard and/or caramelization reactions, coloring the product solution brownish (see also entry 18b, Table 1). The effect is displayed in Figure 2.

Increasing the MeOH-to-H₂O volume ratio in the solvent clearly suppresses the side reactions up to the point, viz. at a solvent volume fraction of 0.8, where the mass-balance is complete (based on GC analysis) and colorless product mixtures are obtained. Notably, DMAE yield increases up to 88 C % in pure MeOH in the presence of Ru. TMEDA (7 C %) and EG (4 C %) are the main byproducts.

Reaction with Different Amines and Effect of Amine-to-GA Ratio in Methanol. As already demonstrated for the GA reaction with DMA in Figure 1, high DMAE yields of 97 C % were obtained in the presence of Pd/C, surprisingly at stoichiometric amine ratio. Reductive amination is thus more selective in MeOH than in water or THF, and therefore it is ideal to revisit the effect of the amine-to-GA molar ratio. Here, the ratio effect of amines such as MMA and NH₃ are investigated for the reductive amination of GA in the presence of Pd/C. DMA concentrations were not varied because high yields of DMAE were already attained at stoichiometric DMA-to-GA ratio in MeOH (vide supra), while no further reaction of the tertiary amine (DMAE) with a new GA molecule is possible, in contrast to the primary products (primary and secondary amines) of reaction of GA with MMA or NH₃. The results are displayed in Figure 3 (top, MMA; bottom, NH₃).

At MMA-to-GA ratios above 3, MAE is the main product with a high 90 C % yield, and a small amount (4 C %) of DMEDA is the main byproduct. Lower ratios result in a gradual increase of EG formation (8 C %, at a ratio value of 0.5), while MAE, being the primary product, further condensates with GA, forming MDEA with an excellent yield of 91 C % at a MMA-to-GA molar ratio of 0.5.

The same experiment with NH₃ at a ratio of 0.33 leads to the formation of 77 C % triethanolamine (TEOA), and changing this molar ratio allows a shift in selectivity towards 70 C % diethanolamine (DEOA) at ratio 5, and substantial MEOA formation at higher NH₃-to-GA molar ratio.

Note that a high mass balance (>95 C %) was measured over the different amine ratios for all reactions, as a result of the promoting effect of MeOH, which is not possible for reactions in aqueous conditions (compare Table 1, entry 1a–b; 4a–d; 9a–b). The chemistry in MeOH tends to form consecutive tertiary amine products, such as TEOA and MDEA in excess of GA, while secondary amines such as MAE and DEOA (or primary amines such as MEOA) are formed in excess of amine in excellent to moderate yield, respectively.

Mechanistic Proposal and Identification of IMs. The above information shows that the selectivity of the catalytic reductive amination of α -OH aldehydes such as GA can strongly be influenced. Parameters such as the solvent, amine type, and ratio play a major role. Here, we propose a general reaction scheme, provided in Scheme 1, for the catalytic reductive amination of GA into C₂ amines. The scheme, which is validated with density functional theory (DFT) calculations, explains all previous observations and product formation and suggests new intermediates, that will be looked at by detailed product (IM) analysis and their evolution in time.

First, the aminating reagent such as NH₃, MMA, and DMA performs a nucleophilic attack on the carbonyl of GA, resulting

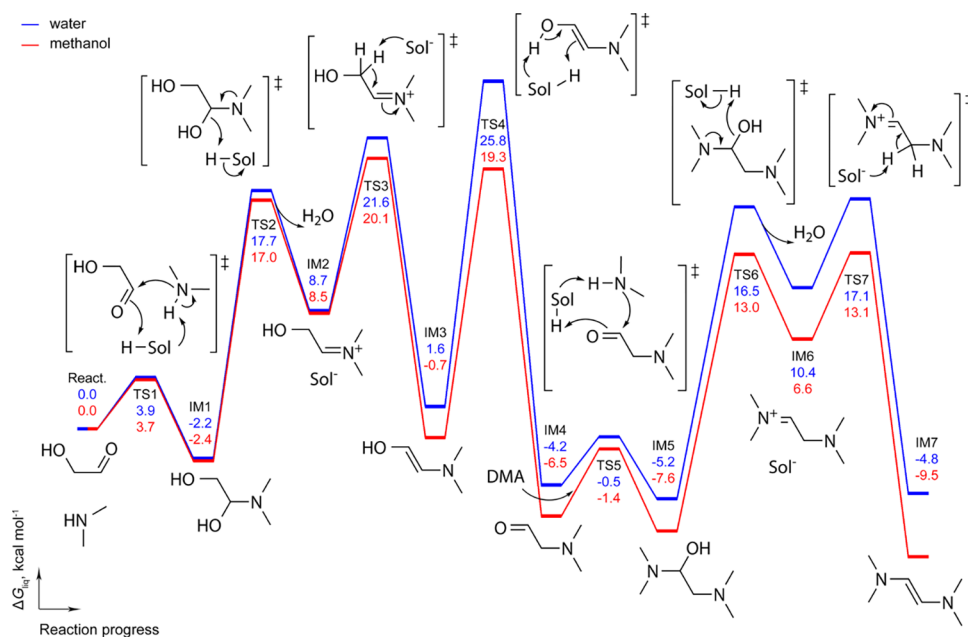


Figure 4. DFT calculated free-energy profile of the reaction between DMA and GA leading to the formation of C₂-ene-diamine intermediate (IM7) in aqueous and in methanol solution.

in the formation of a hemiaminal (IM1), followed by dehydration to an unstable iminium species (IM2). This step is fast with MMA being a strong nonsteric nucleophile, whereas it is slower with NH₃ (less nucleophile) and DMA (more sterically demanding). At the same time, competitive hydrogenation into EG may occur, and this obviously needs to be suppressed, for instance by providing sufficient amount of the amine reagent. Next, an intramolecular PT of IM2 will lead to the stable IM3, which is an imine when the aminating agent is NH₃ or a primary amine such as MMA or an enamine when secondary amines such as DMA are used. Since water is formed, dehydration steps are less obvious in aqueous conditions. IM3 can then be stabilized into the corresponding AAs (5) by means of irreversible hydrogenation, favoring the formation equilibria of IM3. However, when the hydrogenation rate is inadequate such as for Ni when compared to Pd, these components (IM2 and IM3) are susceptible for side reactions, like caramelization and Maillard type of reactions, or IM3 undergoes a base-catalyzed keto–enol tautomerization into its aminoethanal analogue (IM4). This tautomeric form is susceptible to self-condensation to produce heterocyclic piperazines (6) if the amine is not secondary or it reacts with a second amine to form a new hemiaminal IM, and the subsequent C₂-ene-diamine (IM7), and the diamine DA product (8) through subsequent dehydration and hydrogenation steps, respectively. The amine product when primary or secondary can react with another GA molecule, forming higher AAs (9). In excess of GA, the formation of tertiary amine products is favorable.

Energy Barriers and Thermodynamics Using DFT Calculations. The aforementioned mechanism including kinetic and energetic aspects is validated with DFT calculations. In order to obtain atomistic insights into the differences between aqueous and organic solvent conditions, a DFT mechanistic study was first performed with DMA as alkylamine reagent. To rationalize the experimental findings, only the reaction steps prior to catalytic hydrogenation were considered in the DFT study. A mixed explicit/implicit solvent

model was used to assess the effect of the solvent as a mediator on the reaction kinetics and thermodynamics. Inspiration was found in the work of Patil and Sunoj, where the solvent was considered as a proton shuttle for enamine formation.⁵⁷ The free-energy profiles calculated in aqueous and in MeOH media are shown in Figure 4. DFT optimized structures of the species along the reaction paths can be found in Figure S1 of the Supporting Information. Since the structures of the stationary-points located in both solvents are analogous, for the sake of simplicity, the discussion below will be based on the free-energy change calculated in MeOH. The reaction mechanism described here is to a large extent similar to that proposed for the reaction of DMA with reducing sugars, previously published by our group.²⁶ The calculated energy values, however, are not directly comparable because in this study geometry optimizations were carried out in the solvent environment, while gas-phase optimizations were previously used.

In the first reaction step, the DMA nitrogen attacks the carbonyl carbon of GA and the amine proton is transferred (via two solvent molecules) to the substrate carbonyl oxygen through TS1. The energy barrier for this step was calculated to be only 3.7 kcal mol⁻¹. TS1 collapses to a hemiaminal intermediate (IM1) which is thermodynamically preferred over the reactant state by 2.4 kcal mol⁻¹. Next, the hemiaminal compound is converted into the enamine intermediate (IM3) through dehydration. This process passes through two TSs, TS2 and TS3, connected by an unstable iminium intermediate IM2. TS2 corresponds to a proton abstraction from a solvent molecule by the leaving –OH group to form a water product, whereas in TS3 the solvent molecule recovers its proton and a C=C bond is formed in IM3. TS3 is the rate-limiting TS (RLTS) in MeOH media with an energy requirement estimated of 20.1 kcal mol⁻¹. In the following step IM3 is converted into the IM4 tautomer via TS4 of the proton relocation, assisted by three solvent molecules. The free energy of TS4 was calculated to be higher than that of the reactant state by 19.3 kcal mol⁻¹. At this point, hydrogenation to

DMAE can occur to stabilize the product. IM4 can react further with a second DMA molecule, leading to the formation of a C₂-ene-diamine species (IM7), through a TS5–IM5–TS6–IM6–TS7–IM7 mechanism, which is analogous to the previous TS1–IM1–TS2–IM2–TS3–IM3 one. Although the corresponding energy barriers of the distinct reaction steps related with the first and the second DMA addition (e.g. IM1 → TS2 and IM5 → TS6) are similar, the latter should proceed faster because of the energy gain in the formation of IM4. IM7 is the most stable intermediate in this reaction scheme with a free energy estimated lower than that of the reactants by 9.5 kcal mol⁻¹. Both IM3 and IM4 on the one side and IM7 on the other side could be further involved in reactions of catalytic hydrogenation to deliver DMAE and TMEDA products, respectively.

A comparison of the energy profiles obtained in the two solvent environments revealed that MeOH facilitates the amination of GA by increasing both the overall reaction kinetics and the thermodynamic stability of the IM's and products. As can be seen in Figure 4, after the first dehydration step (TS2 and thereafter), the free energy of TS3 and TS4 increases while the stability of IM3 and IM4 decreases (by 2.3 kcal mol⁻¹) in water as compared to MeOH. This tendency is even more pronounced in the second dehydration step (TS6 and thereafter), where the energy of TS6 and TS7 increases by 3–4 kcal mol⁻¹ while the stability of the C₂-ene-diamine product decreases by about 5 kcal mol⁻¹. The difference in the IM stabilities originates from the concentration-dependent contribution to the entropy change which disfavors reactions of water release in aqueous solution. This is accounted for in the calculations by the concentration correction term introduced in eq 1, see section “DFT calculations”.

Another important finding is that in aqueous media the free-energy requirement for keto–enol tautomerization (TS4) increases by 6.5 kcal mol⁻¹ as compared to MeOH and thus it becomes the RLTS. Higher activation energies for keto–enol tautomerization in water than in MeOH were previously reported for other compounds.⁵⁸ As a result, the activation Gibbs function for amination of GA by DMA to C₂-aminoethanal/C₂-ene-diamine product increases from 20.1 kcal mol⁻¹ (TS3) in MeOH to 25.8 kcal mol⁻¹ (TS4) in the aqueous solution.

Study of IM Formation and the Role of the Solvent.

Through experiments and DFT modeling, the solvent effect was found to lower the energy requirement for the RLTS, giving rise to an increased formation rate and more favorable formation (stabilization) of IM's (and products), especially in the case of MeOH. Since it was proposed above that some IM's were relatively stable, their presence in the reaction mixtures should be present during kinetic studies (in absence of the hydrogenation catalysis). To gain additional insights and to confirm the DFT theory, IM product identification and analysis of their evolution in time is carried out in the following section.

Formation of C₂-ene-diamine (IM7). As demonstrated in Table 1, use of Ni catalysis (here Ni-6458P) in water generally led to higher TMEDA selectivity, albeit at a lower total carbon mass balance. Interestingly, when MeOH was used as a solvent and higher amine-to-GA ratio is applied, TMEDA yield increased almost 10-fold to 51 C % with no formation of DMAE.

The evolution of TMEDA formation in function of time is presented in Figure 5. The kinetic data are in full agreement

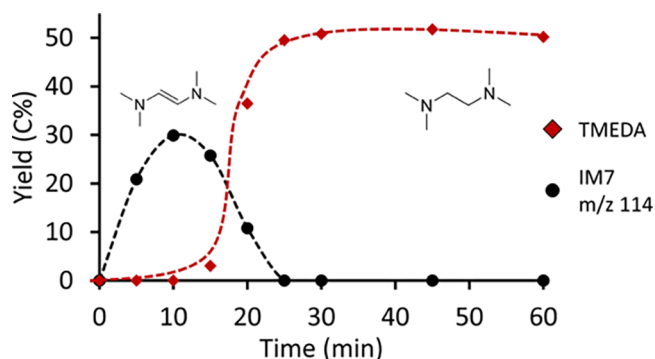


Figure 5. TMEDA and IM formation during the reductive amination of GA. Reaction conditions: 0.5 g GA; 0.4 g Ni-6458P; 0.2 g IS; DMA 2 M in MeOH, diluted to 25 mL total at amine-to-GA molar ratio = 6; 100 °C; 70 bar H₂; 1 h reaction time. Dashed lines are a guide to the eye.

with the theoretical findings: in excess of DMA, DFT calculations predicted TMEDA as the major product of GA amination in MeOH with a yield, higher than that in water. Maximum TMEDA yield was obtained after 30 min, preceded by the formation of a stable IM. Analysis with GC–MS (with parental mass of 114 *m/z*) and ¹³C NMR identified the IM as the C₂-ene-diamine (IM7 in Scheme 1 and Figure 5; more details of identification in Supporting Information, Figures S2 and S3), which is indeed the most stable IM, proposed by the DFT study.

Next, the evolution of IM7 was monitored for reactions in other solvents without the presence of a metal catalyst, at RT with in-line GC analysis. Water has been excluded from this on-line study, and the kinetic data are reported in Figure 6. As

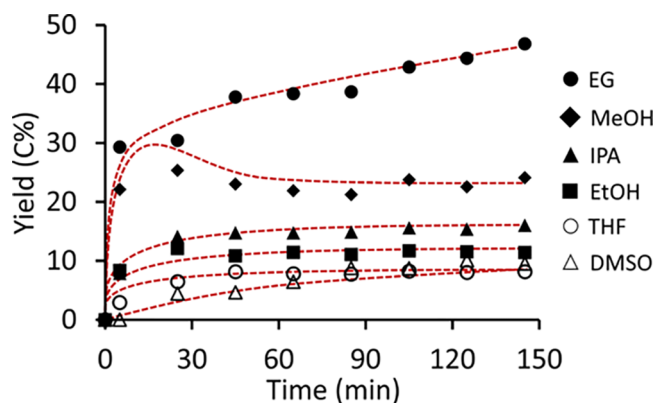


Figure 6. Formation of the TMEDA intermediate IM7 in different solvents at RT. Reaction conditions: 0.05 g GA; 20 μL IS; DMA 2 M in solvent diluted to 1 mL at amine ratio = 3 in a GC vial; on-line GC analysis. Full dots for protic- and hollow dots for aprotic solvents. Dashed lines are a guide to the eye.

can be seen, aprotic polar solvents such as THF and DMSO (hollow dots) gave the lowest IM7 yield, around 10 C %. Alcohols such as isopropanol (IPA), EtOH, and MeOH are slightly better solvents with MeOH reaching a plateau of 22 C % IM7 after 30 min. The most interesting case was the reaction in EG: the formation of IM7 kept increasing, with a yield of 48 C % after 2.5 hours, until a plateau of almost 65 C % was reached after 5 h (not shown here, see Figure S4 in the Supporting Information).

A two-step one-pot experiment, that first led to the formation of IM7 in EG under inert atmosphere, followed by its hydrogenation in the presence of a catalyst under hydrogen pressure, was conducted to check if this effect could be exploited to increase the TMEDA yield. Here, Pd/C was selected as an active hydrogenation catalyst. Because the reaction temperature also affects the tautomerization kinetics toward IM7, reaction at various temperatures was tested. The catalytic results of the two-step approach, applied at different reaction temperature and varying reaction times, are shown in Figure 7.

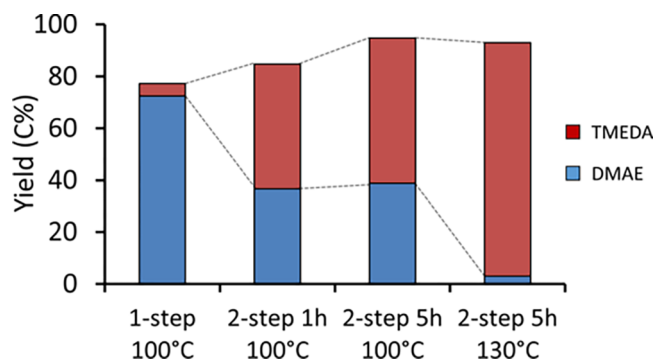


Figure 7. Exploiting the solvent promoting effect by a two-step procedure during the reductive amination of GA. Reaction conditions: 0.5 g GA; 0.5 g Pd/C; 0.2 g IS; DMA in EG, diluted to 25 mL total at amine-to-GA molar ratio = 3 (ratio 12 in case of 130 °C); 0/1/5 h at N₂ 35 bar and RT without catalyst, 1 h at H₂ 70 bar.

As reference, reductive amination of GA with DMA in one-step with Pd/C in EG results in very low TMEDA selectivity. A TMEDA yield well below 10 C % was obtained, while DMAE was formed in high 75% yield. The TMEDA yield increased by 10-fold (to 48 C %) in the two-step approach, already after 1 hour under N₂ and 1 h of hydrogenation reaction conditions. In case the two-step one-pot procedure was allowed for 5 h under inert atmosphere prior to hydrogenation to facilitate IM7 formation, as observed in Figure 6, the TMEDA yield increases to 56 C %. In order to achieve maximum TMEDA selectivity, some improvements were made to the two-step reaction protocol. First, the same reaction protocol at amine-to-GA ratio of 12 (instead of 3) and 5 h reaction time under N₂ conditions further boosted the TMEDA yield to 77 C % (not shown here). Next, the reaction temperature during hydrogenation was increased to 130 °C and this led to a record 91 C % TMEDA yield, the highest reported ever from GA.

Formation of IM6 in the formation of MDEA. Working with MMA or ammonia allows for the formation of (consecutive) higher AAs when lowering the amine-to-GA molar ratio, especially when solvents such as MeOH can help to stabilize the key intermediates (see Figure 3). Formation of intermediates for reaction of GA with MMA was monitored by sampling and GC analysis during the reaction. The product evolution is presented in Figure 8. An initial build-up of an MDEA IM was indeed observed, this time with a prominent *m/z* of 115 feature as determined by GC–MS, followed by the catalytic hydrogenation when the set reaction temperature was reached and a maximum MDEA yield (of 90 C %) after 30 min. The identity of the IM will be discussed later in the text.

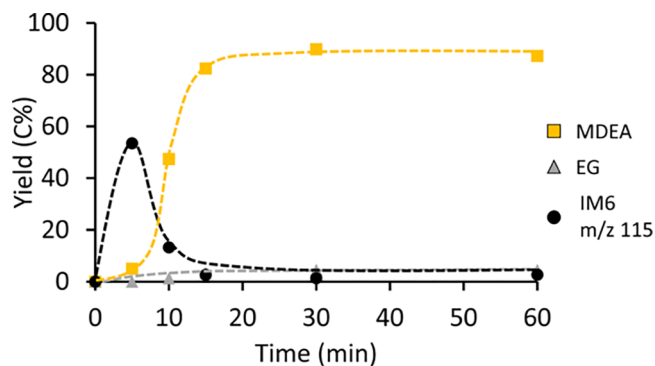


Figure 8. MDEA and IM formation during the reductive amination of GA. Reaction conditions: 1 g GA; 0.4 g Pd/C; 0.2 g IS; MMA 2 M in MeOH, diluted to 25 mL total at amine-to-GA molar ratio = 1/2; 100 °C; 70 bar H₂; 1 h reaction time. Dashed lines are a guide to the eye.

First, similar to the IM7 formation with DMA, the solvent promoting effect on the formation of the unknown MDEA IM was studied by in-line GC analysis for reactions without the metal catalyst and hydrogen pressure in different solvents. The data are presented in Figure 9.

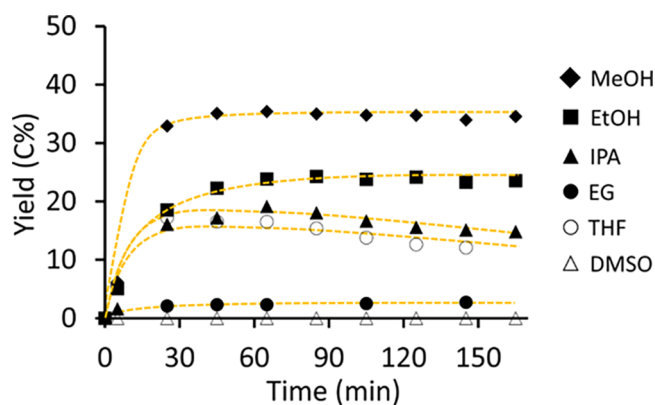
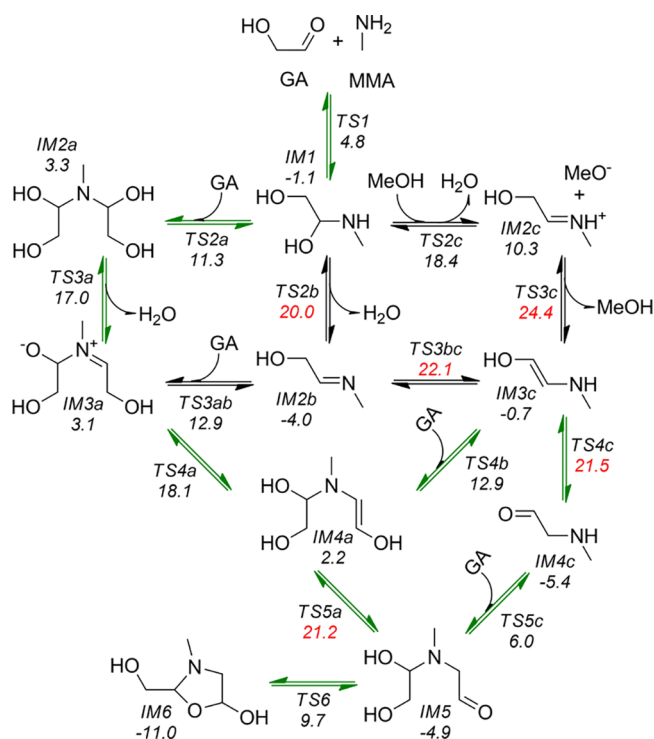


Figure 9. Formation of the MDEA intermediate IM6 in different solvents at RT. Reaction conditions: 0.05 g GA; 20 μL IS; MMA 2 M in solvent diluted to 1 mL at amine-to-GA molar ratio = 1/2 in a GC vial; on-line GC analysis. Full dots for protic and hollow dots for aprotic solvents. Dashed lines are a guide to the eye.

DMSO was the worst solvent in terms of MDEA IM yield (IM6, see Scheme 2), surprisingly followed by EG. Next, IM6 reached a maximum yield in THF and IPA of 17 C % at 30 min after which the IM slowly degraded. This was not the case for EtOH with a steady plateau of 24 C %, followed by MeOH as the best solvent with an IM6 yield of 35 C % at RT.

Parallel to the TMEDA case, the structure of IM6 might at first be an unsaturated MDEA structure, as can be formed in the presence of H₂ but is not expected under N₂ because this route without hydrogenation would create a very reactive and unstable species. Therefore, another hypothesis is proposed, where the addition of a second GA to the *N*-methylaminoethanal leads to the formation of an iminium species (IM3a in Scheme 2), which can undergo a cyclic stabilization in a 5-membered oxazolidinic ring structure (2-(hydroxymethyl)-3-methyloxazolidin-5-ol; IM6, with MW = 133), similar to the proposal of Pelckmans et al.^{25,26} The parental ion of *m/z* = 115 in GC–MS is then formed through fragmentation in the MS with removal of water (MW—18). More details of the MS

Scheme 2. Schematic Presentation of the Reaction between MMA and GA in Methanol Media^a



^aDFT calculated free energies (kcal mol⁻¹) of stationary points, relative to reactant state, are given in *Italic*. The highest TS energies are colored in red. The green arrows show the most likely paths for the formation of the cyclic precursor (IM6) on the free-energy surface.

spectrum and formation of fragments are discussed in the [Supporting Information](#) (see Figures S7–S9).

To provide a mechanistic interpretation of the formation of MDEA, the reaction between MMA and GA was also modeled with DFT methods. The presence of a second proton in the MMA molecule gives rise to a large variety of reaction channels, in addition to that with DMA. Therefore, our DFT modeling was constrained to the cases of MMA-to-GA molar ratio of 1 and 1/2 in MeOH solvent. The resultant reaction network is schematically presented in [Scheme 2](#), and DFT optimized structures of the stationary-points can be found in [Figure S5](#) of the [Supporting Information](#).

Nucleophilic addition of MMA to GA results in the formation of the hemiaminal species, IM1 ([Scheme 2](#)). Further, the reaction can proceed via three competing channels, leading to the formation of (i) IM2a via TS2a of nucleophilic addition of IM1 to a second GA molecule, (ii) imine species IM2b via TS2b, or (iii) enamine species IM3c via TS2c–IM2c–TS3c pathway (by analogy with DMA). According to the calculations, the first reaction channel is more kinetically preferred, as its activation energy is about twice lower than those of the other two channels. Dehydration of IM2a, through TS3a, results in the formation of the zwitterionic intermediate IM3a. The latter can either rearrange to IM4a, through an intramolecular PT in TS4a, or dissociate to imine (IM2b) and GA via TS3ab. Dissociation is more kinetically favorable; however, both the hydration of IM2b back to IM1 (via TS2b) and the tautomerization of IM2b to IM3c (via TS3bc) require higher activation energies than that

calculated for TS4a. IM4a can either tautomerize to IM5, via TS5a, or dissociate to the enamine (IM3c) and GA, via TS4b. Tautomerization of IM3c to IM4c (via TS4c) followed by a nucleophilic addition to a GA molecule (via TS5c) is an alternative route for the formation of IM5. In both cases, the rate for the formation of IM5 is limited by the keto–enol tautomerizations, IM4a ↔ IM5 and IM3c ↔ IM4c, with activation energies of 21.2 (TS5a) or 21.5 (TS4c) kcal mol⁻¹, respectively. Finally, intramolecular attack of the hemiaminal –OH group on the carbonyl C-atom of IM5 results in the formation of a five-membered oxazolidinic ring structure IM6. The energy requirement for this step was estimated at 9.7 kcal mol⁻¹, being the most stable intermediate ($\Delta G_{\text{liq}} = -11.0$ kcal mol⁻¹) in this reaction scheme, followed by IM4c ($\Delta G_{\text{liq}} = -5.4$ kcal mol⁻¹), IM5 ($\Delta G_{\text{liq}} = -4.9$ kcal mol⁻¹), and IM2b ($\Delta G_{\text{liq}} = -4.0$ kcal mol⁻¹). Thus, the calculations predict the cyclic oxazolidine precursor as the major product under thermodynamic control and excess of GA, which is in agreement with the experimental data.

To finally support the product identification of IM6, ¹³C NMR and GC–MS was applied. The DFT-calculated ¹³C NMR chemical shifts of IM6 are in excellent agreement with the experimental NMR spectrum, thus confirming the structural identity of this compound (Figures S7–S9 of the [Supporting Information](#)).

When using equimolar amounts of the reactants; however, the C₂-aminoethanal compound (IM4c) is expected to be the major species in MeOH solution. The catalytic hydrogenation of IM4c results directly in the MAE product, whereas the formation of MDEA from IM6 is less obvious since IM6 is a saturated compound. According to the calculations, IM6, IM5, and IM4c are in fast equilibrium. The latter two (being unsaturated) can be involved further in reactions of hydrogenation to deliver MDEA, as suggested in [Figure S6](#) of the [Supporting Information](#).

Valorization of Bio-based MDEA-Esterquat. All of the components produced herein have an industrial application, and therefore, amination of GA may serve as an interesting alternative replacing EO and EDC. For example, MDEA on itself is a promising solvent for CO₂-capture,⁵⁹ but it can also be used as a substrate in, for example, the production of esterquats for fabric softeners as demonstrated in [Figure 10](#). It is well known that MDEA-esterquats are a good alternative to TEA-based esterquats (herein also produced from GA), in terms of both biodegradability and cost/performance. The MDEA esterquats reduce the surface tension of water, are biodegrade in 2 days, and have a function as a bacteriostatic agent.³ However, in order to shift toward a sustainable economy with daily consumer chemicals, it is important that households experience no loss in their living standard using alternative building blocks, thus having high performance. Via the route presented here, esterquats could have the potential to be biobased if produced from GA as a drop-in and ultimately close the carbon cycle.

To demonstrate the applicability of our bio-based route as a proof of concept, MDEA and BHEDMEDA diester quats (the latter obtained from Pelckmans et al.²⁶) were synthesized from the obtained reaction mixtures, formulated into a fabric softener and tested on standardized towels against an industrial TEA standard fabric softener (structure see [Figure S13](#) in [Supporting Information](#)) and a blank.

A sensory assessment was performed by a panel of trained people, to rank the conditioned towels from soft to hard, and a

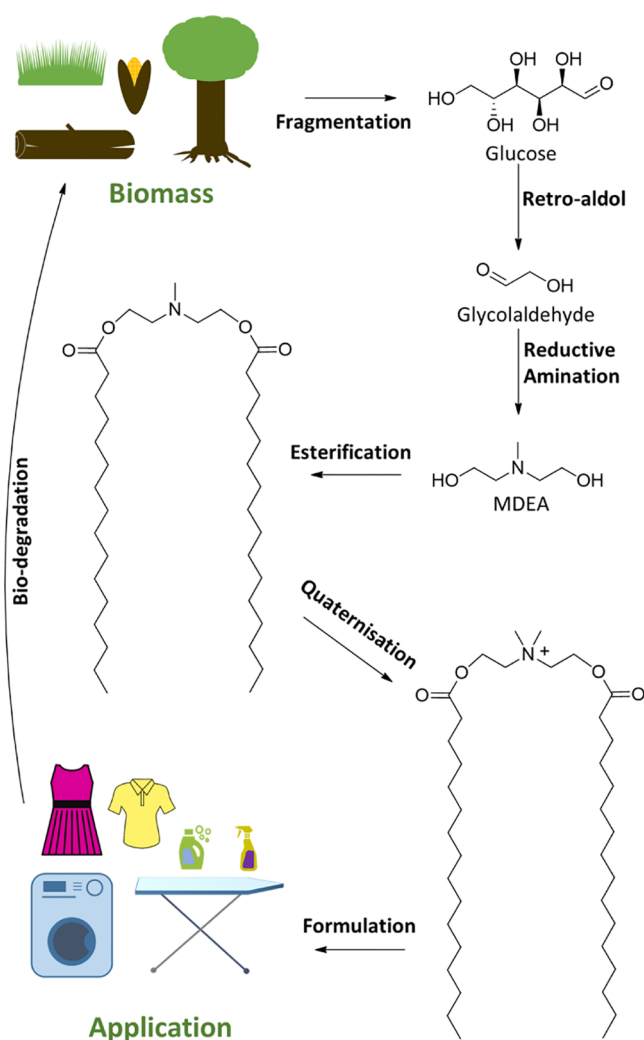


Figure 10. Overall route for the synthesis and application of bio-based MDEA esterquats.

statistical approach was conducted to reach a conclusion on their performance (see [Supporting Information](#)). Based on these results, performance of the esterquats were ranked as follows with a 95% significance: MDEA > TEA > BHEDMEDA > blank. Most importantly, all esterquats were found to have softening properties compared to the blank formulation. Furthermore, it was demonstrated that the bio-based MDEA can indeed be used as a bio-based drop-in for esterquat formulations with high softening performance, without impacting the quality. Although BHEDMEDA led to a very similar structure, having a double quaternary ammonium head instead of a single, a significant ($P < 0.05$) loss in softening performance was observed. It is assumed that the double charge on the molecule has great impact on its adsorption properties toward fibers, which will not be discussed in detail here.

DISCUSSION AND CONCLUSION

To prove GA as alternative, non-toxic and safer substrate for C_2 amine synthesis, the challenge was found in understanding the different parameters that control product selectivity. Being a reactive molecule, the amination pathway towards AA and DA products needs to be facilitated above the undesired hydrogenation (EG formation) and condensation (oligomer

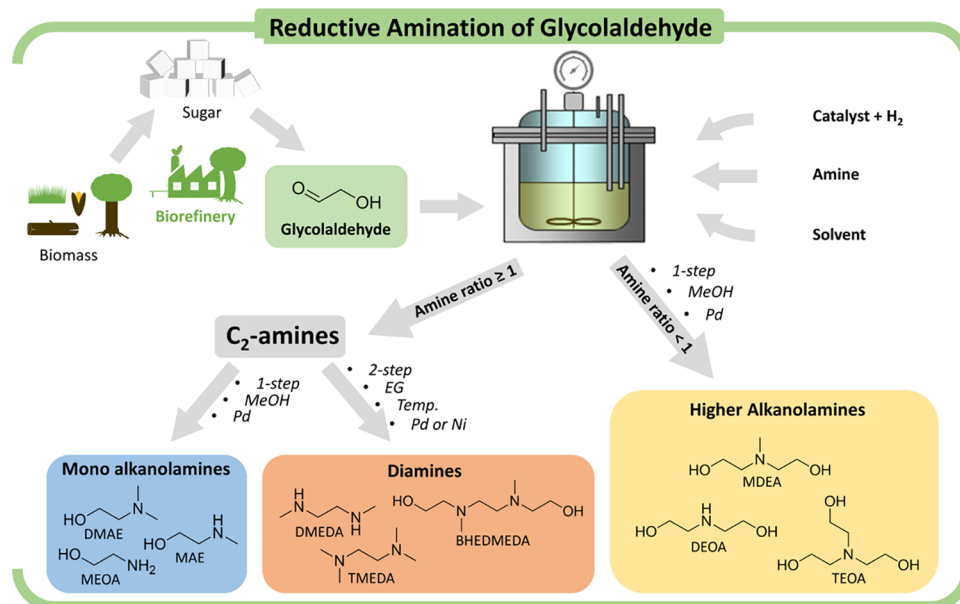
formation) reactions. As demonstrated for aqueous conditions in [Table 1](#), a high amine excess is required for the reaction but with varying results depending on the amine reagent. High yield is possible with MMA being a strong non-steric nucleophile, but only poor results are obtained with NH_3 (less nucleophile) and DMA (sterically more demanding). In contrast, use of other solvents, showed to be of major importance to unlock high mass balance and product selectivity.

While dehydration steps in formation of the hemiaminal are hindered in water ([Scheme 1](#)), the use of organic solvents to provide a “dehydrating environment” is more favorable. It was long thought that inert organic solvents such as THF were ideal to create these nonaqueous conditions.⁵⁴ However, use of organic protic solvents such as MeOH show much better AA yields, irrespective of the amine reagent, as demonstrated in [Figures 1–3](#). Solvent-dependent DFT calculations suggest both thermodynamic (IM and product stability) and kinetic aspects (lower energy barriers due to occurrence of fast PT) that facilitate the reaction channels toward reductive amination, see [Figure 4](#), thus suppressing the undesired side reactions. Because of the occurrence of fast PT, protic solvents such as MeOH thus cannot be considered to be inert.^{26,56,57} As a result, GA reductive amination in MeOH results in close to quantitative AA formation such as MAE (from MMA) and DMAE (from DMA), and excess of amine reagent to achieve high product yield is not necessary anymore. Only the reaction of GA with NH_3 still benefits of an excess amine reagent to obtain moderate MEOA yield, as consecutive reactions are more readily possible here.

Controlling (sub)-stoichiometric amounts of amine to GA demonstrated the formation of valuable higher (secondary and tertiary amine) AAs, see [Figure 3](#), and their overall mass balance is always very high in contrast to those obtained in water or THF. This observation in MeOH is explained by the fast condensation of the primary and secondary amine IMs in the reaction mechanism with another GA molecule, allowing the formation of MDEA (91 C %) (with MMA) and DEOA (70 C %) and TEOA (77 C %) (with NH_3). Detailed product analysis and kinetics (exemplified for the reaction of GA with MMA) revealed the dominant formation of a stable peculiar intermediate IM6. This cyclic oxazolidine precursor is in equilibrium with little amounts of other (linear unsaturated) intermediates, as demonstrated in [Figures 8 and 9](#) and [Scheme 2](#) and leads to the higher AA product. To the best of our knowledge, this is the first proof that a variety of bio-based AAs can be catalytically produced in one step with such high yield, starting from GA as the substrate. This is primarily enabled by the solvent and by means of a similar process approach as the common EO production process, that is changing the selectivity of AAs upon different amine-to-substrate ratios. However in contrast with EO, the use of GA at comparable molar amine-to-substrate ratios gives considerably better yields of the higher AAs such as MDEA, DEOA, and TEOA.¹

Further catalyst development will be helpful to improve the versatility of this process. Highly active metal catalysts such as Pd (and Ru) are preferred as they rapidly convert the imine (or enamine) into the stable amine end product. As such, AAs are the main products in the presence of these noble catalysts. In order to shift toward DA (ethylene diamine)-selective reactions, tautomerization should occur prior to hydrogenation. Slower hydrogenation, for instance, by using Ni (instead of noble metals), and high amine-to-GA ratio favor

Scheme 3. Routes toward Bio-Based AAs and Ethylene Diamines



chemoselectivity toward DA. Other options worth to explore further are the use of less catalyst and lowering of the hydrogen pressure. Detailed product analysis and kinetics, in Figures 5 and 6, clearly revealed the formation of a C₂-ene-diamine (IM7). DFT calculations in Scheme 2 found this IM to be 5.7 kcal mol⁻¹ more stable in MeOH, originating from the favorable entropy change of dehydration in nonaqueous conditions. Simultaneously, lowest energy barriers were encountered in MeOH, as the RLTS shifts to TS3 with a decrease of 6.5 kcal mol⁻¹ compared to water.

Figure 7 then demonstrated that IM7 formation can be further optimized by utilizing EG as a solvent. An experimental NIR spectroscopy study already evidenced that EG–water interactions are stronger in water-poor mediums than those obtained in bulk water.⁶⁰ DFT and ab initio study on model clusters also showed that the EG–water interaction is dominant over the EG–EG and water–water interactions.⁶¹ Given the above, processes associated with the release of water will thus be favored, to some extent, in EG media. To check these assumptions, we have optimized the key TSs along the reactions of DMA (TS2, TS3, and TS4) with GA, and have compared the resultant energies with those obtained in MeOH. DFT-optimized structures are given in Figure S10 of the Supporting Information. Indeed, the relative free energy of TS2, corresponding to the first water release in the reaction of DMA with GA, decreases from 17.0 kcal mol⁻¹ in MeOH to 12.8 and kcal mol⁻¹ in the EG solvent. An energy decrease of 1 kcal mol⁻¹ was also obtained for TS3 of proton abstraction (which is the RLTS in MeOH), but in contrary, the relative Gibbs energy of TS4 (keto–enol tautomerization) slightly increases, from 19.3 in MeOH to 21.1 kcal mol⁻¹ in EG solvent, as it now becomes the RLTS in EG media. As the differences in energy values are however comparable to the accuracy of the computational methods, their results should only be discussed qualitatively. Overall, as the calculations predict a slightly higher activation energy for the reaction between DMA and GA in EG (TS4, 21.1 kcal mol⁻¹) compared to MeOH (TS3, 20.1 kcal mol⁻¹), the experimental results primarily evidenced for faster kinetics of IM7 formation

in EG solvent. Use of higher temperature successfully compensated the slower tautomerization in EG, yielding large amounts of IM7 in an inert atmosphere. This stable formation is exploited successfully in a one-pot two-step approach to form TMEDA in almost quantitative yield: first, IM7 is formed in EG under an inert atmosphere, followed by pressurizing the reactor with hydrogen for the reductive amination. We believe that this approach can be further explored with other secondary amine reagents (such as MAE) to form interesting and novel DAs (such as BHEDMEDA), and work is in progress here.

In summary, the first conceptual model toward bio-based AAs and ethylene diamines (DAs) from GA is presented in Scheme 3, demonstrating possible routes to drop-in and novel C₂ amines straight from GA. As α -OH substrates such as GA show high reactivity in reductive amination reactions, this work demonstrated the mechanistic insights into its chemistry and solvent effect in order to obtain a high mass balance with optimum product selectivity. To illustrate the potential, a MDEA-based diester quat was successfully prepared and formulations were tested in a sensory assessment, proving the viability for a bio-based production of high-value chemicals starting from GA as platform, while being biodegradable and therefore ultimately closing the carbon cycle.

■ ASSOCIATED CONTENT

Additional ¹³C NMR and GC–MS spectra, DFT-optimized geometries, pathway for MDEA formation, listing of catalyst properties, test panel results on washing softener: hierarchy, and pair-wise tests (PDF)

■ AUTHOR INFORMATION

Corresponding Author

*E-mail: bert.sels@kuleuven.be. Phone: +32 16 32 15 93.

ORCID

Kristine Pierloot: 0000-0002-3196-4940

Bert F. Sels: 0000-0001-9657-1710

Notes

The authors declare no competing financial interest.

ACKNOWLEDGMENTS

W.F. and M.P. acknowledge the Flemish government for their financial support in the Carboleum icon project of Catalisti. The computational resources and services used in this work were provided by the Flemish Supercomputer Center, funded by the Hercules Foundation and the Flemish Government-department EWI. The calculations were performed on the HPC cluster Tier-2 of KU Leuven. B.F.S. acknowledges the C₂ project of KULeuven on bio-based amines.

ABBREVIATIONS

DMAE, 2-(dimethylamino)ethanol; MDEA, *N*-methyl-diethanolamine; BHEDMEDA, *N,N'*-bis(2-hydroxyethyl)-*N,N'*-dimethyl-ethylenediamine; MAE, 2-(methylamino)ethanol; MEOA, monoethanolamine; DEOA, diethanolamine; TEOA, triethanolamine; GA, glycolaldehyde; EG, ethylene glycol; TMEDA, *N,N,N',N'*-tetramethylethylenediamine; DMEDA, *N,N'*-dimethylethylenediamine; EO, ethylene oxide; DCE, dichloroethane; IM, intermediate; AA, alkanolamine; DA, diamine; NH₃, ammonia; MMA, monomethylamine; DMA, dimethyl amine; MeOH, methanol; EtOH, ethanol; THF, tetrahydrofuran; IPA, iso-propanol; 3EGDE or IS, triethylene glycol dimethyl ether; DMSO, dimethylsulfoxide; TMS, tetramethylsilane; RT, room temperature; GC, gas-chromatography; GCMS, gas-chromatography coupled with mass-spectrometry; NMR, nuclear magnetic resonance analysis; DFT, density functional theory; TS, transition state; RLTS, rate-limiting transition state; PT, proton transfer

REFERENCES

- (1) Frauenkron, M.; Melder, J.-P.; Ruider, G.; Rossbacher, R.; Höke, H. Ethanolamines and Propanolamines. *Ullmann's Encyclopedia of Industrial Chemistry*; Wiley-VCH, 2012; Vol. 405–528.
- (2) Idem, R.; Wilson, M.; Tontiwachwuthikul, P.; Chakma, A.; Veawab, A.; Aroonwilas, A.; Gelowitz, D. Pilot Plant Studies of the CO₂ Capture Performance of Aqueous MEA and Mixed MEA/MDEA Solvents at the University of Regina CO₂ Capture Technology Development Plant and the Boundary Dam CO₂ Capture Demonstration Plant. *Ind. Eng. Chem. Res.* **2006**, *45*, 2414–2420.
- (3) Han, B.; Geng, T.; Jiang, Y.; Ju, H. Synthesis and Properties of Di-Chain Esterquat Surfactants. *J. Surfactants Deterg.* **2015**, *18*, 91–95.
- (4) Bremecker, K.-D.; Natonski, J. L.; Eachus, A. C. The role of primary alkanolamines in cosmetic formulation. *Int. J. Cosmet. Sci.* **1991**, *13*, 235–247.
- (5) Calignano, A.; La Rana, G.; Piomelli, D. Antinociceptive activity of the endogenous fatty acid amide, palmitylethanolamide. *Eur. J. Pharmacol.* **2001**, *419*, 191–198.
- (6) Roose, P.; Eller, K.; Henkes, E.; Rossbacher, R.; Höke, H. Amines, Aliphatic. *Ullmann's Encyclopedia of Industrial Chemistry*; Wiley-VCH, 2015; Vol. 1–55.
- (7) Mohsenzadeh, A.; Zamani, A.; Taherzadeh, M. J. Bioethylene Production from Ethanol: A Review and Techno-economical Evaluation. *ChemBioEng Rev.* **2017**, *4*, 75–91.
- (8) Pelckmans, M.; Renders, T.; Van de Vyver, S.; Sels, B. F. Bio-based amines through sustainable heterogeneous catalysis. *Green Chem.* **2017**, *19*, 5303–5331.

(9) Garcia, C. L.; Darroudi, F.; Bates, A. D.; Natarajan, A. T. Induction and persistence of micronuclei, sister-chromatid exchanges and chromosomal aberrations in splenocytes and bone-marrow cells of rats exposed to ethylene oxide. *Mutat. Res.* **2001**, *492*, 59–67.

(10) Murphy, M. J.; Dunbar, D. A.; Kaminsky, L. S. Acute toxicity of fluorinated ether anesthetics: role of 2,2,2-trifluoroethanol and other metabolites. *Toxicol. Appl. Pharmacol.* **1983**, *71*, 84–92.

(11) de Haan, A. B.; Meindersma, G. W.; Nijenstein, J.; Vitasari, C. A Techno-Economic Evaluation on the Feasibility of Chemicals from Pyrolysis Oil. *Nordic Wood Biorefinery Conference*, 2011.

(12) Vitasari, C. R.; Meindersma, G. W.; de Haan, A. B. Laboratory scale conceptual process development for the isolation of renewable glycolaldehyde from pyrolysis oil to produce fermentation feedstock. *Green Chem.* **2012**, *14*, 321.

(13) Sasaki, M.; Goto, K.; Tajima, K.; Adschiri, T.; Arai, K. Rapid and selective retro-aldol condensation of glucose to glycolaldehyde in supercritical water. *Green Chem.* **2002**, *4*, 285–287.

(14) Wang, A.; Zhang, T. One-Pot Conversion of Cellulose to ethylene glycol with multifunctional Tungsten-Based Catalysts. *Acc. Chem. Res.* **2013**, *46*, 1377–1386.

(15) Zhang, J.; Hou, B.; Wang, A.; Li, Z.; Wang, H.; Zhang, T. Kinetic Study of Retro-Aldol Condensation of Glucose to Glycolaldehyde with Ammonium Metatungstate as the Catalyst. *AIChE J.* **2014**, *60*, 3804–3813.

(16) Majerski, P. A.; Piskorz, J. K.; Radlein, D. S. A. G. Production of glycolaldehyde by hydrous thermolysis of sugars; U.S. Patent 7,094,932 B2, 2006.

(17) Taarning, E. process for removing formaldehyde from a composition comprising glycolaldehyde; WO2014131743A1. 28, 2014.

(18) Schreck, D.; Chrisman, R.; Brooke, A.; Clinton, N. process for the continuous production of ethylene glycol from carbohydrates; WO2015179302A1, 2015.

(19) Ji, N.; Zhang, T.; Zheng, M.; Wang, A.; Wang, H.; Wang, X.; Shu, Y.; Stottlemeyer, A. L.; Chen, J. G. Catalytic conversion of cellulose into ethylene glycol over supported carbide catalysts. *Catal. Today* **2009**, *147*, 77–85.

(20) Cao, Y.; Wang, J.; Kang, M.; Zhu, Y. Catalytic conversion of glucose and cellobiose to ethylene glycol over Ni–WO₃/SBA-15 catalysts. *RSC Adv.* **2015**, *5*, 90904–90912.

(21) Ooms, R.; Dusselier, M.; Geboers, J. A.; Op de Beeck, B.; Verhaeven, R.; Gobechiya, E.; Martens, J. A.; Redl, A.; Sels, B. F. Conversion of sugars to ethylene glycol with nickel tungsten carbide in a fed-batch reactor: high productivity and reaction network elucidation. *Green Chem.* **2014**, *16*, 695–707.

(22) Marup Osmundsen, C.; Taarning, E.; Larsen, M. B. Process for the preparation of ethylene glycol from sugars; WO2017118701A1, 2017.

(23) Haldor Topsoe. Bio-based chemicals one step closer to commercial breakthrough [Press release]. <https://blog.topsoe.com/bio-based-chemicals-one-step-closer-to-commercial-breakthrough>, 2017.

(24) Haldor Topsoe. Braskem and Haldor Topsoe start up demo unit for developing renewable MEG. <https://blog.topsoe.com/braskem-and-haldor-topsoe-start-up-demo-unit-for-developing-renewable-meg>. 2019.

(25) Pelckmans, M.; Vermandel, W.; Van Waes, F.; Moonen, K.; Sels, B. F. Low-Temperature Reductive Aminolysis of Carbohydrates to Diamines and Aminoalcohols by Heterogeneous Catalysis. *Angew. Chem., Int. Ed.* **2017**, *56*, 14540–14544.

(26) Pelckmans, M.; Mihaylov, T.; Faveere, W.; Poissonnier, J.; Van Waes, F.; Moonen, K.; Marin, G. B.; Thybaut, J. W.; Pierloot, K.; Sels, B. F. Catalytic Reductive Aminolysis of Reducing Sugars: Elucidation of Reaction Mechanism. *ACS Catal.* **2018**, *8*, 4201–4212.

(27) Liang, G.; Wang, A.; Li, L.; Xu, G.; Yan, N.; Zhang, T. Production of Primary Amines by Reductive Amination of Biomass-Derived Aldehydes/Ketones. *Angew. Chem., Int. Ed.* **2017**, *56*, 3050–3054.

- (28) Han, Y.; Zhang, J.; Liu, X. Molybdenum-containing acidic catalysts to convert cellulosic biomass to glycolic acid. U.S. Patent 8,846,974 B2, 2014.
- (29) Holm, M. S.; Saravanamurugan, S.; Taarning, E. Conversion of Sugars to Lactic Acid Derivatives Using Heterogeneous Zeotype catalysts. *Science* **2010**, *328*, 602–605.
- (30) Dusselier, M.; van Wouwe, P.; De Smet, S.; De Clercq, R.; Verbelen, L.; Van Puyvelde, P.; Du Prez, F. E.; Sels, B. F. Toward Functional Polyester Building Blocks from Renewable Glycolaldehyde with Sn Cascade Catalysis. *ACS Catal.* **2013**, *3*, 1786–1800.
- (31) Orazov, M.; Davis, M. E. Tandem catalysis for the production of alkyl lactates from ketohexoses at moderate temperatures. *Proc. Natl. Acad. Sci. U.S.A.* **2015**, *112*, 11777–11782.
- (32) Luebben, S. D.; Raebiger, J. W. A Novel Renewable Thermoplastic Polyacetal by Polymerization of Glycolaldehyde Dimer, a Major Product of the Fast Pyrolysis of Cellulosic Feedstock. *Green Polymer Chemistry: Biobased Materials and Biocatalysis*; ACS Publication, 2015; pp 305–328.
- (33) Tolborg, S.; Meier, S.; Saravanamurugan, S.; Fristrup, P. Shape-selective Valorization of Biomass-derived Glycolaldehyde using Tin-containing Zeolites. *ChemSusChem* **2016**, *9*, 3021.
- (34) Wang, A.; Liang, G.; Zhang, T. Method for Preparing Ethanolamine and Diamine by Glycolaldehyde Reductive Amination 107,011,194 A, 2017.
- (35) Trégnier, T. Reductive Amination of 1-Hydroxy-2-propanone Over Nickel and Copper Catalysts. *Chem. Biochem. Eng. Q.* **2018**, *31*, 455–470.
- (36) Gomez, S.; Peters, J. A.; Maschmeyer, T. The Reductive Amination of Aldehydes and Ketones and the Hydrogenation of Nitriles: Mechanistic Aspects and Selectivity Control. *Adv. Synth. Catal.* **2002**, *344*, 1037–1057.
- (37) Nursten, H. E. *The Maillard reaction: Chemistry, biochemistry and implications*; RSC Food Analysis Monographs, 2005.
- (38) Kroh, L. W. Caramelisation in foods and beverages. *Food Chem.* **1994**, *51*, 373–379.
- (39) Hodge, J. E. The Amadori Rearrangement. *Adv. Carbohydr. Chem.* **1955**, *10*, 169–205.
- (40) Pérez, P.; Toro-Labbé, A. Theoretical analysis of some substituted imine-enamine tautomerism. *Theor. Chem. Acc. Theory Comput. Model.* **2001**, *105*, 422–430.
- (41) Weissmehl, K.; Arpe, H.-J. *Industrial Organic Chemistry*; Wiley-VCH, 2008.
- (42) Winans, C. F. Method of preparing secondary amines. U.S. Patent 2,217,630 A, 1940.
- (43) Scanlon, J. T.; Willis, D. E. Calculation of flame ionization detector relative response factors using the effective carbon number concept. *J. Chromatogr. Sci.* **1985**, *23*, 333–340.
- (44) Zhao, Y.; Truhlar, D. G. The M06 suite of density functionals for main group thermochemistry, thermochemical kinetics, non-covalent interactions, excited states, and transition elements: two new functionals and systematic testing of four M06-class functionals and 12 other functionals. *Theor. Chem. Acc.* **2008**, *120*, 215–241.
- (45) Frisch, M. J.; Trucks, G. W.; Schlegel, H. B.; Scuseria, G. E.; Robb, M. A.; Cheeseman, J. R.; Scalmani, G.; Barone, V.; Mennucci, B.; Petersson, G. A.; Nakatsuji, H.; Caricato, M.; Li, X.; Hratchian, H. P.; Izmaylov, A. F.; Bloino, J.; Zheng, G.; Sonnenberg, J. L.; Hada, M.; Ehara, M.; Toyota, K.; Fukuda, R.; Hasegawa, J.; Ishida, M.; Nakajima, T.; Honda, Y.; Kitao, O.; Nakai, H.; Vreven, T.; Montgomery, J. A., Jr.; Peralta, J. E.; Ogliaro, F.; Bearpark, M.; Heyd, J. J.; Brothers, E.; Kudin, K. N.; Staroverov, V. N.; Keith, T.; Kobayashi, R.; Normand, J.; Raghavachari, K.; Rendell, A.; Burant, J. C.; Iyengar, S. S.; Tomasi, J.; Cossi, M.; Rega, N.; Millam, J. M.; Klene, M.; Knox, J. E.; Cross, J. B.; Bakken, V.; Adamo, C.; Jaramillo, J.; Gomperts, R.; Stratmann, R. E.; Yazyev, O.; Austin, A. J.; Cammi, R.; Pomelli, C.; Ochterski, J. W.; Martin, R. L.; Morokuma, K.; Zakrzewski, V. G.; Voth, G. A.; Salvador, P.; Dannenberg, J. J.; Dapprich, S.; Daniels, A. D.; Farkas, O.; Foresman, J. B.; Ortiz, J. V.; Cioslowski, J.; Fox, D. J. *Gaussian 09*, 2013.
- (46) Cancès, E.; Mennucci, B.; Tomasi, J. A new integral equation formalism for the polarizable continuum model: Theoretical background and applications to isotropic and anisotropic dielectrics. *J. Chem. Phys.* **1997**, *107*, 3032–3041.
- (47) Mennucci, B.; Cancès, E.; Tomasi, J. Evaluation of Solvent Effects in Isotropic and Anisotropic Dielectrics, and in Ionic Solutions with a Unified Integral Equation Method: Theoretical Bases, Computational Implementation and Numerical Applications. *J. Phys. Chem. B* **1997**, *101*, 10506–10517.
- (48) Pliego, J. R., Jr.; Riveros, J. M. A Theoretical Analysis of the Free-Energy Profile of the Different Pathways in the Alkaline Hydrolysis of Methyl Formate In Aqueous Solution. *Chem.—Eur. J.* **2002**, *8*, 1945–1953.
- (49) Sunoj, R. B.; Anand, M. Microsolvated transition state models for improved insight into chemical properties and reaction mechanisms. *Phys. Chem. Chem. Phys.* **2012**, *14*, 12715–12736.
- (50) Bryantsev, V. S.; Diallo, M. S.; Goddard, W. A., III Calculation of Solvation Free Energies of Charged Solutes Using Mixed Cluster/Continuum Models. *J. Phys. Chem. B* **2008**, *112*, 9709–9719.
- (51) Chandrashekar, V.; Srujan, M.; prabhakar, R.; Reddy, R. C.; Sreedhar, B.; Rentam, K. K. R.; Kanjilal, S.; Chaudhuri, A. Cationic amphiphiles with fatty acyl chain asymmetry of coconut oil deliver genes selectively to mouse lung. *Bioconjug. Chem.* **2011**, *22*, 497–509.
- (52) De Vos, N. *Development of New Ionic Liquids Based on a 7-aza- or 7-thiabicyclo(2.2.1) Heptane Skeleton*; Ghent University, 2013.
- (53) Kramer, A.; Kahan, G.; Cooper, D.; Papavasiliou, A. A Non-parametric Ranking Method for the Statistical Evaluation of Sensory Data. *Chem. Senses Flavor* **1974**, *1*, 121–133.
- (54) Mägerlein, W.; Melder, J.-P.; Pastre, J.; Eberhardt, J.; Krug, T.; Kreitschmann, M. Reaction of glycolaldehyde with an aminating agent. U.S. Patent 8,772,548 B2, 2012.
- (55) Poissonnier, J.; Pelckmans, M.; Van Waes, F.; Moonen, K.; Sels, B. F.; Thybaut, J. W.; Marin, G. B. Kinetics of homogeneous and heterogeneous reactions in the reductive aminolysis of glucose with dimethylamine. *Appl. Catal., B* **2018**, *227*, 161–169.
- (56) Song, S.; Wang, Y.; Yan, N. A remarkable solvent effect on reductive amination of ketones. *Mol. Catal.* **2018**, *454*, 87–93.
- (57) Patil, M. P.; Sunoj, R. B. Insights on co-catalyst-promoted enamine formation between dimethylamine and propanal through ab initio and density functional theory study. *J. Org. Chem.* **2007**, *72*, 8202–8215.
- (58) Arslan, N. B.; Ozdemir, N. Direct and solvent-assisted keto-enol tautomerism and hydrogen-bonding interactions in 4-(m-chlorobenzylamino)-3-phenyl-4,5-dihydro-1H-1,2,4-triazol-5-one: a quantum-chemical study. *J. Mol. Model.* **2015**, *21*, 19.
- (59) Closmann, F.; Nguyen, T.; Rochelle, G. T. MDEA/Piperazine as a solvent for CO₂ capture. *Energy Procedia* **2009**, *1*, 1351–1357.
- (60) Chen, Y.; Ozaki, Y.; Czarnecki, M. A. Molecular structure and hydrogen bonding in pure liquid ethylene glycol and ethylene glycol-water mixtures studied using NIR spectroscopy. *Phys. Chem. Chem. Phys.* **2013**, *15*, 18694.
- (61) Kumar, R. M.; Baskar, P.; Balamurugan, K.; Das, S.; Subramanian, V. On the Perturbation of the H-Bonding Interaction in Ethylene Glycol Clusters upon Hydration. *J. Phys. Chem. A* **2012**, *116*, 4239–4247.